고성능 응답을 위한 유도 전동기의 근사적 비간섭 제어

°김 동일, 고 명삼, 하 인중, 박 재화
서울대학교 공과대학 제어계측공학과

Asmptotic Decoupled Control of Induction Motors for High Dynamic Performance

Dong-Il Kim, Myoung-Sam Ko, In-Joong Ha, and Jae-Hwa Park

Deptpartment of Control and Instrumentation Engineering
Seoul National University

Abstract

An attractive approach to speed of induction motors is to achieve full linearization via appropriate feedback.However, the prior results toward this direction are based on full feedback. In practice, rotor fluxes are not directly measurable but can be estimated using observers. We propose a nonlinear feedback controller with an observer. As $t \to \infty$, the closed-loop system with our controller becomes as if it were a linearly decoupled system. We provide the stability analysis of our control method. Simulation and experimental results are also included to demonstrate the practical significance of our results.

1.Introduction

The recent rapid growth in microprocessor technologies facilitates application of computationally complex control methods to be applied in many industrial problems. Since the so called vector control pioneered by Blaschke (1972), there have been a number of notable researches toward high dynamic performance of induction motors. For instance, they are (Gabriel 1980, Sugimoto 1983, Brod 1985, Harashima 1985, Kuroe 1986, Koyama 1986, Ohnishi 1986, Lorenz 1987). The underlying idea of their control methods is to make the induction motor behave like a DC motor by controlling the rotor fluxes constant. A good survey on induction motor control is found in (Leonhard 1986).

Along with remarkable advances in nonlinear feedback control theory (Jakubczyk 1980, Isidori 1981, 1985, Hunt 1983, Nijmeier 1983, Ha 1986, 1988), its recent results have been successfully applied to induction motors (Krzeminski 1987, Luca 1987) and other electric machines (Marino 1984, Illic'-Spong 1987). In this approach, the nonlinear dynamic equations of the induction motor are transformed into a linear system via appropriate nonlinear feedback. Then, well-known results in linear control theory are employed.

In this paper, we attempt to achieve high performance dynamic response by means of decoupled control of rotor speed and flux. Recently developed nonlinear feedback control theories are utilized. Our approach differs from the prior works in the following aspects. While the prior results are promising and have their own merits, full state feedback is required (Krzeminski 1987, Luca 1987) or full linearization is not obtained (Harashima 1985, Kuroe 1986, Koyama 1986, Ohnishi 1986). In practice, rotor fluxes can be measured directly through flux-coils or hall-probes (Blaschke 1972, Plunkett 1977). However, it is more cost-effective to estimate rotor fluxes based on the rotor circuit equations (Garcés 1980, Koyama 1986, Hori 1987). Motivated by the prior results, we construct a nonlinear feedback controller with an observer estimating rotor flux. After sufficient time of motor operation, the speed dynamic chracteristics of the induction motor with our controller become linear. Thereby, we achieve high performance dynamic response. This is made possible by decoupled control of rotor speed and flux.

We provide the stability analysis of the closed-loop system with our controller. Both simulation and experimental results are included to demonstrate the practical significance of our result. In particular, our experimental results contribute to showing that recently developed nonlinear feedback control techniques are of practical use.

2.Main Result

The dynamic equations of an induction motor with p pole pairs can be written in the d-q coordinate system rotating synchronously with an angular speed w_s as

$$\dot{i}_{ds} = -a_1 i_{ds} + w_s i_{qs} + a_2 \phi_{dr} + p a_3 w_r \phi_{qr} + cV_{ds}$$

$$\dot{i}_{qs} = -w_s i_{ds} - a_1 i_{qs} - p a_3 w_r \phi_{dr} + a_2 \phi_{qr} + cV_{qs}$$

$$\dot{\phi}_{dr} = -a_4 \phi_{dr} + a_5 i_{ds} + (w_s - p w_r)\phi_{qr}$$

$$\dot{\phi}_{qr} = -a_4 \phi_{qr} + a_5 i_{qs} - (w_s - p w_r)\phi_{dr} \tag{2.1}$$

$$\dot{w}_r = \frac{(-Bw_r + T_e - T_L)}{J}, \tag{2.2}$$

where T_e is the generated torque given by

$$T_e = K_T(\phi_{dr} i_{qs} - \phi_{qr} i_{ds}). \tag{2.3}$$

Here, V_{ds}, V_{qs}, w_s are the control inputs available to controller designers and a_i, $i=1,..,5$ are the parameters of the induction motor. Definitions of the symbols used frequently in the developments are given in Nomenclature.

First, we describe our controller for the induction motors characterized by the above (2.1)-(2.3). Our controller has the form:

$$u = \begin{bmatrix} V_{ds} \\ V_{qs} \end{bmatrix} = \begin{bmatrix} -\dfrac{w_s i_{qs}}{c} + \hat{u}_1 \\ \dfrac{p w_r (i_{ds} + a_3 \hat{\phi}_{dr})}{c} + \dfrac{\hat{u}_2}{\hat{\phi}_{dr}} \end{bmatrix}, \tag{2.4}$$

where $\hat{\phi}_{dr}$ is obtained by the observer:

$$\dot{\hat{\phi}}_{dr}=-a_4\hat{\phi}_{dr}+a_5 i_{ds}, \tag{2.5}$$

and

$$w_s=pw_r+a_5\frac{i_{qs}}{\hat{\phi}_{dr}}. \tag{2.6}$$

For successful set-point tracking, $\Omega=[\Omega_1\ \Omega_2]^T$ is chosen as

$$\Omega_1=-K_{c\phi}i_{ds}-K_{p\phi}\hat{\phi}_{dr}+K_{i\phi}\int_0^t(\phi_{dr}^*-\hat{\phi}_{dr})dt,$$

$$\Omega_2=-K_{cw}\hat{\phi}_{dr}i_{qs}-K_{pw}w_r+K_{iw}\int_0^t(w_r^*-w_r)dt. \tag{2.7}$$

Here, ϕ_{dr}^*, w_r^* are the reference set points for ϕ_{dr}, w_r, respectively. In the next theorem, we shall prove that as $t\rightarrow\infty$, i) the closed-loop system described by (2.1)-(2.3) and (2.4)-(2.7) behaves as if it were a linear decoupled system and ii) $\phi_{dr}\rightarrow\phi_{dr}^*$, $\phi_{qr}\rightarrow 0$, and $w_r\rightarrow w_r^*$. Before stating our theorem, some discussions would be helpful for readers to catch up the main idea of our approach.

Let $x\triangleq[x_1\cdots x_8]^T$ where $x_1\triangleq i_{ds}$, $x_2\triangleq\phi_{dr}$, $x_4\triangleq i_{qs}$, $x_5\triangleq w_r$, $x_7\triangleq\phi_{qr}$, and $x_8\triangleq\hat{\phi}_{dr}$. Let $u^*\triangleq[\phi_{dr}^*\ \ w_r^*]^T$ and $y\triangleq[\phi_{dr}\ \ w_r]^T$. Then, the closed-loop system given by (2.1)-(2.7) can be written as

$$\dot{x}=F(x)+G(x)u^*+HT_L,\ y=Lx, \tag{2.8}$$

where the detailed structures of F, G, H, and L are given in Appendix A. The dynamic behavior of the system (2.8) is hard to be analyzed in its present form. For this reason, the following state transformation is introduced. Let $w\triangleq[z\ \ e]^T$, $z\triangleq[z_1\cdots z_6]^T$ and $e\triangleq[e_1\ \ e_2]^T$. In the new coordinate system of state variables defined by the system (2.8) is represented as

$$\dot{w}=\begin{bmatrix}\dot{z}\\ \dot{e}\end{bmatrix}=\begin{bmatrix}Az+f(w)e+Bu^*+\hat{H}T_L\\ h(w)e\end{bmatrix},$$
$$y=Cz, \tag{2.10}$$

where the detailed structures of f, h, A, B, $\hat{H}$, and C are given in Appendix A. Note that the input-output dynamic characteristics of (2.10) are the same as those of (2.8) since only the state transformation (2.9) is involved between two systems (2.8) and (2.10).

Now, we discuss the special case of $e\equiv 0$ in (2.10). The system (2.10) is then reduced to the decoupled linear system:

$$\dot{z}_m=Az_m+Bu^*+\hat{H}T_L,$$
$$y_m=Cz_m. \tag{2.11}$$

The block diagram representation of (2.11) is shown in Fig.2.1. From Fig.2.1, we see that when $\hat{\phi}_{dr}=\phi_{dr}$ and $\phi_{qr}=0$ can be accomplished, the controller in (2.4) and (2.6) plays the role of linearizing fully the dynamic equations of the induction motor in (2.1)-(2.3) with its input-output dynamic behavior decoupled, while the controller in (2.7) provides the linearly decoupled system with desirable dynamic characteristics. In this case, ϕ_{dr} and w_r can be independently controlled and are dynamically uncoupled . Furthermore, when u^* and T_L are constant, it is assured that $|y-u^*|\rightarrow 0$ as $t\rightarrow\infty$. Hence, in the case of $e\equiv 0$, the controller in (2.4)-(2.7) allows for stably decoupled control of rotor speed and flux.

The following theorem tells that as $t\rightarrow\infty$, $|y-y_m|\rightarrow 0$. That is, as $t\rightarrow\infty$, the input-output dynamic characteristics of nonlinear system (2.8) resemble those of the decoupled linear system (2.11). Hence, the closed-loop system (2.10) eventually possesses all advantages described for the case of $e\equiv 0$ in the preceding paragraph.

Theorem 2.1 Suppose that

(A.1) A is a stable matrix.
(A.2) For each $u^*:[0,\infty)\rightarrow\Omega_1\times\Omega_2$ and $T_L:[0,\infty)\rightarrow\Omega_T$ and $x(0)\in\Omega_x$ the system (2.8) has a unique solution $x:[0,\infty)\rightarrow\Omega_x$.

Then, the controller given by (2.4)-(2.7) guarantees that

$$|y-y_m|\rightarrow 0 \text{ and } \phi_{qr}\rightarrow 0 \text{ as } t\rightarrow\infty \tag{2.12}$$

In addition, if u^* and T_L are constant,

$$|y-u^*|\rightarrow 0 \text{ as } t\rightarrow\infty \tag{2.13}$$

Proof

Let $Q\in R^{6\times 6}$ be a positive definite symmetric matrix. By (A.1), there exists a positive definite matrix $P\in R^{6\times 6}$ satisfying

$$A^TP+PA=-Q \tag{2.14}$$

Let

$$\phi(w)\triangleq f(w)e \tag{2.15}$$

Since T in (2.9) is a compact mapping, $T(\Omega_x)$ is a compact subset of R^8. Furthermore, f is continuous on $T(\Omega_x)$. By this observation and (A.2), there exists $\alpha>0$ such that

$$|\phi(w)|\leq\alpha|e| \tag{2.16}$$

Choose $\gamma>0$ so that

$$2a_4\lambda_m(Q)>\alpha^2\gamma\|P\|^2 \tag{2.17}$$

Let

$$\Lambda=\begin{bmatrix}2a_4 & -\alpha\gamma\|P\|\\ -\alpha\gamma\|P\| & \gamma\lambda_m(Q)\end{bmatrix} \tag{2.18}$$

Note that by (2.17), Λ is positive definite. Let $e_m\triangleq z-z_m$. From (2.10) and (2.11), we obtain

$$\dot{e}_m=Ae_m+\phi(w)$$
$$\dot{e}=h(w)e \tag{2.19}$$

$$y-y_m=Ce_m \tag{2.20}$$

Define a Lyapunov-like function V by

$$V=e^Te+\gamma e_m^TPe_m \tag{2.21}$$

Then, it follows from (2.14), (2.16), and (2.19) that

$$\dot{V}=-2a_4e^Te-\gamma e_m^TQe_m+2e_m^TP\phi(w)\gamma$$
$$\leq-2a_4|e|^2-\gamma\lambda_m(Q)|e_m|^2+2\gamma\alpha|e_m|\|P\||e|$$
$$=-[|e|\,|e_m|]\Lambda[|e|\,|e_m|]^T \tag{2.22}$$
$$\leq-\lambda_m(\Lambda)|[e^T e_m^T]^T|^2$$

By (2.17),

$$\lambda_m(\Lambda)>0 \tag{2.23}$$

By (2.21)-(2.23), we can conclude that (2.12) is true. Finally, suppose that T_L and u^* are constant. Then, it easily follows that from Fig.2.1 and (A.1) that

$$|y_m-u^*|\rightarrow 0 \text{ as } t\rightarrow\infty \tag{2.24}$$

On the other hand,

$$|y-u^*| \le |y-y_m| + |y_m-u^*| \qquad (2.25)$$

This with (2.12) and (2.24) proves (2.13).

We need some comments on the assumptions (A.1) and (A.2). From Fig.2.1, we see that (A.1) can be always satisfied by appropriate choice of the controller gains, $K_{I\phi}$, $K_{P\phi}$, $K_{C\phi}$, K_{Iw}, K_{Pw}, and K_{Cw}. The assumption (A.2) is needed for simplicity of proof. It can be removed by imposing restrictions on the allowable sizes of $\Omega_1 \times \Omega_2$, Ω_T, and $|x(0)|$. Then, the proof of Theorem 2.1 becomes more complicated. Moreover, (2.12) and (2.13) hold locally rather than globally.

Finally, we discuss at some length the prior results related to our controller in the following remarks.

Remark 2.1 During the preparation of this paper, the very recent paper by (Krzeminski 1987) came up to our attention. We should note that he is the first person to find a controller which provides decoupled control of rotor speed and flux for the special case of $\phi_{dr}=\hat{\phi}_{dr}$ and $\phi_{qr}=0$. However, our theorem is still new. In (Krzeminski 1987), the rotor fluxes are assumed to be measurable and any experiments were not performed. Other notable results on decoupled control can be found in (Sugimoto 1983, Harashima 1985, Kuroe 1986, Koyama 1986, Ohnishi 1986). The controller in (Kuroe 1986) forces the induction motor dynamics to behave like a linear system as $t \to \infty$. However, the controllers in (Sugimoto 1983, Harashima 1985, Kuroe 1986, Koyama 1986, Ohnishi 1986) do not completely decouple the rotor speed and flux .

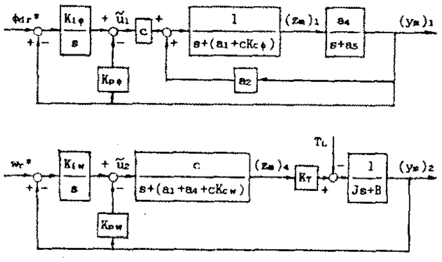

Fig.2.1. The block diagram of the decoupled linear system (2.11).

3. Simulations and Experiments

The practical use of our controller developed in the preceding section is examined through simulations and experiments. The tested induction motor is a squirrel cage type with 4 poles, rated power 2.2 kW, and rated speed 1750 rpm. The nominal values of its parameters are listed in table 3.1. The controller gains used in the simulations and experiments are

$$K_{P\phi} = 104.295 \quad K_{I\phi} = 1210.0 \quad K_{C\phi} = 3.0$$
$$K_{Pw} = 0.424 \quad K_{Iw} = 1.997 \quad K_{Cw} = 0.522 \qquad (3.1)$$

Before presenting simulation and experimental results, we describe the microprocessor-based control system used as a test bed for our controller. As is shown in Fig.3.1, it consists of a 16 bit microprocessor (Motolora 68000) with the CPU clock rate of 8 MHz, a 3 kW peak rated PWM inverter, and the pre-described squirrel cage induction motor. Signals between the microprocessor and the induction motor are processed through 12bit A/D converters, D/A converters, and 682_1 peripheral interface adapters. The rotor speed and position are detected by 6840 counter/timers and an optical encoder whose resolution is 4000 pulses/rev. The DC generator with rated power 2.2 kW and rated speed 1750 rpm was coupled with the induction motor for the load test.

Table 3.1. Nominal parameters of the tested induction motor.

220V/380V, 60Hz, Delta-Connected Stator			
R_s	0.687Ω	R_r	0.842Ω
L_s	83.97mH	L_r	85.28mH
M	81.36mH	J	0.03Kgm²
B	0.01Kgm²/s	σ	0.0756
i_{ds}(rated)	5.9A	i_{qs}(rated)	11A

The 2ϕ-3ϕ coordinate transformation in Fig.3.1 is required to convert the control inputs for d-q axis stator voltages into those for the actual phase voltages. It is given by

$$\begin{bmatrix} V_{as} \\ V_{bs} \\ V_{cs} \end{bmatrix} = \begin{bmatrix} \sin\theta_s & \cos\theta_s \\ -\sin(\theta_s+\pi/3) & -\sin(\theta_s-\pi/6) \\ -\sin(\theta_s-\pi/3) & -\sin(\theta_s+\pi/6) \end{bmatrix} \begin{bmatrix} V_{ds} \\ V_{qs} \end{bmatrix} \qquad (3.2)$$

where $\theta_s = \int w_s dt$.

On the other hand, the 3ϕ-2ϕ coordinate transformation is to convert the measured stator phase currents into the corresponding values in the rotating d-q coordinate system. It is given by

$$\begin{bmatrix} i_{ds} \\ i_{qs} \end{bmatrix} = \begin{bmatrix} \sin(\theta_s-\pi/6) & -\cos\theta_s \\ \sin(\theta_s+\pi/3) & \sin\theta_s \end{bmatrix} \begin{bmatrix} i_{as} \\ i_{bs} \end{bmatrix} \qquad (3.3)$$

The overall control algorithm composed of (2.4)-(2.7), (2.26), (3.2), and (3.3) is executed every 0.5ms on the Motolora 68000 microprocessor.

In the simulation, the controller given by (2.4)-(2.7) is considered. The command senario of ϕ_{dr}^* and w_r^* is selected as follows. At 0.4 sec, w_r^* is switched from 800 rpm to 1200 rpm, while ϕ_{dr}^* is switched from 0.244 Wb to 0.48 Wb. Then, ϕ_{dr}^* is switched back to 0.244 Wb at 1.5 sec. The simulation and exeperimental results shown in Fig.3.2(a) and Fig.3.3(a) demonstrate that the controller given by (2.4)-(2.7) successfully decouples responses of the rotor flux and rotor speed. Also, a rated torque 12 Nm is applied from 0.4 sec until 1.4 sec, while ϕ_{dr}^*, w_r^* are set 0.48 Wb, 800 rpm, respectively. The simulation and experimental results are shown in Fig.3.2(b) and Fig.3.3(b). While the rotor speed response recovers its commanded value promptly, the rotor response is not affected by the load torque.

As can be seen from Fig.3.2-Fig.3.3, the experimental results agree well with the simulation results. However, our experimental results reveal weak coupling between responses of ϕ_{dr} and w_r. In practice, it is difficult to achieve complete decoupled control of ϕ_{dr} and w_r mainly because of two reasons. First, the control algorithm is performed through 16 bit word operations in the microprocessor, so there exist quantization errors, roundoff errors, and truncation errors. Second, there exist mismatches between the actual parameters of the induction motor and those used in the simulations. Such parameter uncertainties may arise from magnetic saturation, change of temperature, and so on.

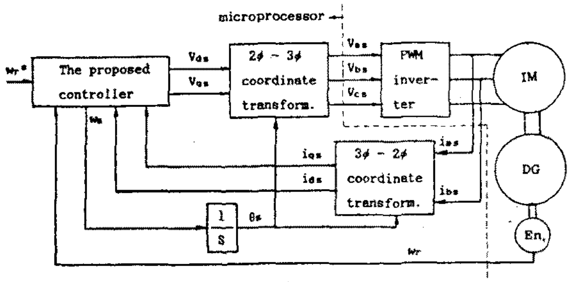

Fig.3.1. Configuration of the control system.

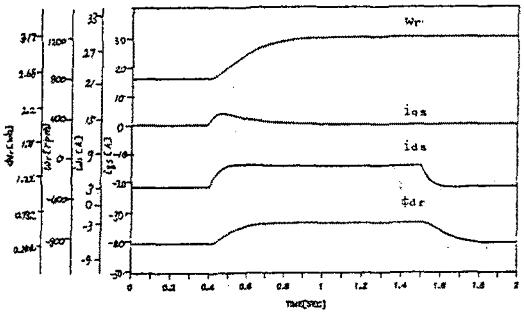

(a) Responses for a step command of w_r^* and rectangular command of ϕ_{dr}^*.

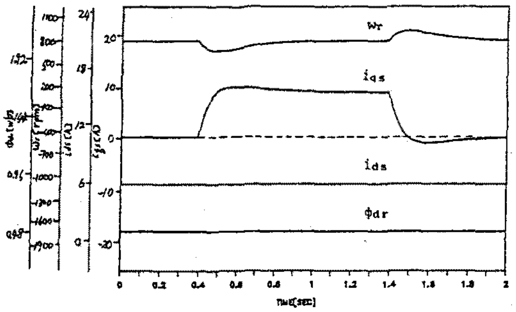

(b) Responses for rectangular load torque.

Fig.3.2. Simulation results for the controller given by (2.4)-(2.7).

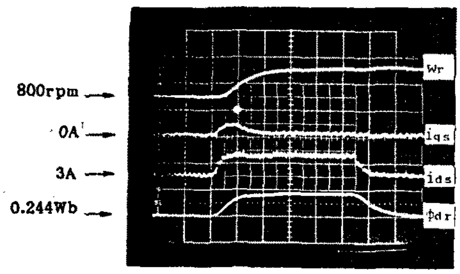

w_r :400rpm/div. i_{qs}:5A/div. i_{ds}:3.6A/div. ϕ_{dr}:0.3Wb/div. x-axis:0.2sec/div.

(a) Responses for a step command of w_r^* and rectangular command of ϕ_{dr}^*.

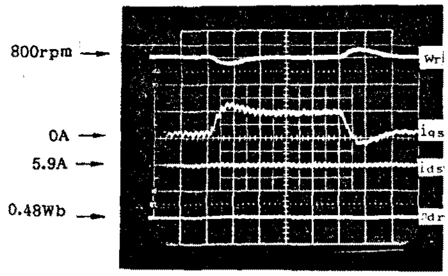

w_r :600rpm/div. i_{qs}:10A/div. i_{ds}:3A/div. ϕ_{dr}:0.3Wb/div. x-axis:0.2sec/div.

(b) Responses for a rectangular load torque.

Fig.3.3. Experimental results for the controller given by (2.4)-(2.7).

4.Conclusion

Through simulations and experiments, we have shown that the proposed control method can be effectively used in induction motor control to achieve high dynamic performance. Comparison of the simulation and experimental results affirms that the proposed control method is robust against modelling uncertainties. However, aging effect or high temperature may bring in large modelling uncertainties and, in turn, can degenerate its performance badly. Further research should be directed toward improving the proposed method in the respects of computational load and robustness against large modelling uncertainties.

Acknowledgement

This work was supported by Gold Star Industrial Systems Coorperation Ltd..The authors would like to thank Yong-Ho Kim, Dr. Kye-Young Lim, and Dr. Ho-Hyun Choe in Gold Star Industrial Systems Coorperation Ltd. for their numerous helpful suggestions during this work.

Nomenclature

V_{ds} (V_{qs})	d-axis (q-axis) stator voltage
V_a (V_b, V_c)	stator phase voltages
i_{ds} (i_{qs})	d-axis (q-axis) stator current
ϕ_{dr} (ϕ_{qr})	d-axis (q-axis) rotor flux
w_r	rotor angular speed
w_{sl}	slip angular speed
R_s (R_r)	stator (rotor) resistance
L_s (L_r)	stator (rotor) self-inductance
M	stator/rotor mutual inductance
p	the number of pole pairs
σ	$1-M^2/L_sL_r$:leakage coefficient
c	$1/\sigma L_s$
a_1	$c(R_s+M^2R_r/L_r^2)$
a_2	cMR_r/L_r^2
a_3	cM/L_r
a_4	R_r/L_r
a_5	MR_r/L_r
J	rotor inertia of MG set
B	damping coefficient of MG set
T_L	torque disturbance
$\|x\|$	the Euclidean norm of $x \in R^n$
$\Omega_1 \times \Omega_2$	a compact subset of R^2
Ω_x	a compact subset of R^8 such that $\Omega_x \cap \{x \in R^8 : x_2 = x_8 = 0\} = \phi$
$\lambda_m(M)$	the minimum eigenvalue of a symmetric matrix M

Appendix A

(1) F, G, H, and L in (2.8):

$$F(x)=\begin{bmatrix} -(a_1+cK_{c\phi})x_1+a_2x_2+cK_{i\phi}x_3-cK_{p\phi}x_8+pa_3x_5x_7 \\ a_5x_1-a_4x_2+a_5\dfrac{x_4x_7}{x_8} \\ -x_8 \\ -(a_1+cK_{cw})x_4+a_2x_7-pa_3x_5(x_2-x_8)-\dfrac{a_5x_1x_4+c(K_{pw}x_5-K_{iw}x_6)}{x_8} \\ -\dfrac{Bx_5}{J}+\dfrac{K_T(x_2x_4-x_1x_7)}{J} \\ -x_5 \\ a_5x_4-a_4x_7-a_5\dfrac{x_2x_4}{x_8} \\ a_5x_1-a_4x_8 \end{bmatrix},$$

$$G(x)=\begin{bmatrix} 0&0&1&0&0&0&0&0 \\ 0&0&0&0&0&1&0&0 \end{bmatrix}^T, H=\begin{bmatrix} 0&0&0&0&\dfrac{1}{J}&0&0&0 \end{bmatrix}^T, L=\begin{bmatrix} 0&1&0&0&0&0&0&0 \\ 0&0&0&0&1&0&0&0 \end{bmatrix}.$$

(2) A, B, C, and $\widehat{H}$ in (2.10):

$$A=\left[\begin{array}{ccc|ccc} -(a_1+cK_{c\phi}) & a_2-cK_{p\phi} & cK_{i\phi} & 0 & 0 & 0 \\ a_5 & -a_4 & 0 & 0 & 0 & 0 \\ 0 & -1 & 0 & 0 & 0 & 0 \\ \hline 0 & 0 & 0 & -(a_1+a_4+cK_{cw}) & -cK_{pw} & cK_{iw} \\ 0 & 0 & 0 & \dfrac{K_T}{J} & -\dfrac{B}{J} & 0 \\ 0 & 0 & 0 & 0 & -1 & 0 \end{array}\right],$$

$$\widehat{H}^T=\left[\begin{array}{ccc|ccc} 0&0&0&0&-\dfrac{1}{J}&0 \end{array}\right], B^T=\left[\begin{array}{ccc|ccc} 0&0&1&0&0&0 \\ 0&0&0&0&0&1 \end{array}\right], C^T=\left[\begin{array}{ccc|ccc} 0&1&0&0&0&0 \\ 0&0&0&0&1&0 \end{array}\right],$$

$$f(w)=\left[\begin{array}{c|c} pa_3z_5 & cK_{p\phi} \\ \dfrac{a_5z_4}{z_2(z_2-e_2)} & 0 \\ 0 & 1 \\ \hline \dfrac{a_5z_4^2}{z_2^2(z_2-e_2)}+a_2z_2 & \dfrac{cz_2(K_{iw}z_6-K_{pw}z_5)-a_5z_1z_4}{z_2(z_2-e_2)}-pa_3z_2z_5 \\ -\dfrac{K_T}{J}z_1 & 0 \\ 0 & 0 \end{array}\right],$$

$$h(w)=\left[\begin{array}{c|c} -a_4 & \dfrac{-a_5z_4}{z_2(z_2-e_2)} \\ \hline \dfrac{a_5z_4}{z_2(z_2-e_2)} & -a_4 \end{array}\right].$$

References

Blaschke, F., 1972, Simens Review, **34**, 217.

Brod, D. M. and Novotny, D, W., 1985, *I.E.E.E. Trans. Ind Appl.*,**21**, 562.

Gabriel, R. et al., 1980, *I.E.E.E. Trans. Ind. Appl.*, **16**, 186.

Garcés, L. J., 1980, *I.E.E.E. Trans. Ind. Appl.*, **16**, 173.

Ha, I. J. and Gilbert, E. G., 1986 *I.E.E.E. Trans. Automat. Contr.*, **31**, 823.

Ha, I. J., 1988, *will appear in SIAM J. Contr. and Optim.*, **26**, 1.

Harashima, F. et al., 1985, *I.E.E.E. Trans. Ind. Appl.*, **21**, 602.

Hori, Y. et al., 1987, *10th IFAC Conference*, **3**, 355.

Hunt, L. R. et al., 1983, *I.E.E.E. Trans. Automat. Contr.*, **28**, 24.

Illic'-Spong, M. et al., 1987, *I.E.E.E. Trans. Automat. Contr.*, **32**, 371.

Isidori, A. et al., 1981, *I.E.E.E. Trans. Automat. Contr.*, **26**, 331.

Isidori, A., 1985, *Nonlinear Control Systems: An Introduction* (New York: Springer-Verlag)

Jakubczyk, B. and Respondeck, W., 1980, *Bull. Acad. Pol. Sci. Math.*, **28**, 517.

Krzeminski, Z., 1987, *10th IFAC Conference*, **3**, 349.

Kuroe, Y. and Haneda, H., 1986, *Proceeding of the 25th CDC*, 54.

Leohnard, W., 1986, *Automatica*, **22**, 1.

Lorenz, R. D. and Lawson, D. B., 1987, *I.E.E.E. Trans. Ind. Appl.*, **23**, 597.

Luca, A. D. and Ulivi, G., 1987, *Proceeding of the 26th CDC*, 1765.

Marino, R. 1984, *I.E.E.E. Trans. Automat. Contr.*, **29**, 276.

Nijmeijer, H., 1983, *I.E.E.E. Trans. Automat. Contr.*, **28**, 861.

Mutoh, N. et al., 1986, *I.E.E.E. Trans. Ind. Elec.*, **33**, 52.

Ohnishi, K. et al., 1985, *I.E.E.E. Trans. Ind. Appl.*, **21**, 241.

Plunkett, A. B., 1977, *I.E.E.E. Trans. Ind. Appl.*, **13**, 139.

Plunkett, A. B. et al.,1985, *I.E.E.E. Trans. Ind. Appl.*, **21**, 456.

Sugimoto, H., 1983, *International Power Electronics Con.*, 462.